Available online at www.sciencedirect.com
SCIENCE DIRECT®
Polymer 44 (2003) 3935–3943
polymer
www.elsevier.com/locate/polymer

Liquid-crystalline elastomers produced by chemical crosslinking agents containing sulfonic acid groups

Fanbao Meng, Baoyan Zhang*, Lumei Liu, Baoling Zang

Department of Chemistry, Research Centre for Molecular Science and Engineering, Northeastern University, 110004 Shenyang, People's Republic of China

Received 17 September 2002; received in revised form 24 February 2003; accepted 25 March 2003

Abstract

A series of siloxane-based liquid-crystalline (LC) elastomers were synthesized by using chemical crosslinking agents containing sulfonic acid groups. The crosslink densities of the elastomers were determined by swelling experiments. Two kinds of melting temperature corresponding to crystallization of siloxane matrix and crystallization of LC segments were clearly detected. Some of the polymers exhibited smectic mesophase textures or cholesteric mesophase textures. A proposed model containing LC segment structure and ionic crosslinking lamellar structure separated by siloxane chains was given. The ion aggregated in domains forces the siloxane chains to fold and form an irregular lamellar structure. Ionic aggregates and LC segments may be dispersed each other to form multiple blocks with increasing ionic crosslinking content.

Keywords: Liquid-crystalline elastomers; Ionic crosslinking agents; Sulfonic acid

1. Introduction

Liquid-crystalline (LC) elastomers have received a lot of interest during recent years owing to their special optical, mechanical and piezoelectric properties [1–3]. The polymer network structure of the LC elastomers is usually produced by the introduction of crosslinking into LC polymer systems. This crosslinking results in materials with a number of unusual properties.

Recently, some work has been devoted to the functionalization of LC polymers with ionic groups. The interest in this class of polymer stems from the attempt to combine the ionic clustering of classical ionomers (leading to physical crosslinking for example) with the formation of LC phases [4–6]. The ionic groups are incorporated either into the molecular backbone or on side-chains to improve the physical properties and water dispersibility of hydrophobic organic polymers [7]. Ionic aggregates can play a role in physical crosslinking and provide an important and characteristic viscoelastic behavior of ionomers. The incorporation of small concentration of ions into organic polymers has been shown to lead to microphase-separated ionic domains that influence greatly the properties of the polymers. In fact, the LC ionomers show a combination of the properties of liquid crystals and ionomers [8]. On the one hand, they exhibit a behavior analogous to that of isotropic ionomers, i.e. the formation of clusters of ionic groups that belong to different polymer chains. This results in the gelation of the polymer and the formation of a temporary network structure. On the other hand, the liquid crystallinity gives rise to an organization by ordering of mesogenic fragments.

However, little work has been reported on the effect of chemical crosslinking agents containing ionic groups on the properties of LC networks.

One would like to know the fundamental link between ionic aggregation found in the networks and the behavior of LC phases. For LC ionomers, it has been shown that ionic clustering and physical gelation is compatible with LC phases [9–11]. It is interesting to investigate the relationship between ionic clusters and LC phases in ionic LC elastomers. Furthermore, it is also interest to investigate how the ionic interactions and crosslinking agents modify liquid crystallinity, LC structure, and properties of such kind of elastomers.

In the present study, we prepared a series of LC elastomers using chemical crosslinking agents containing

* Corresponding author. Fax: +86-24-8368-7446.
E-mail address: baoyanzhang@hotmail.com (B. Zhang).

0032-3861/03/$ - see front matter © 2003 Elsevier Science Ltd. All rights reserved.
doi:10.1016/S0032-3861(03)00271-4

ionic groups, which were siloxane-based materials. Their general structure is shown in Scheme 1. Elastomers of this type may be readily prepared in a one-step reaction, in which both the mesogenic unit and an ionic divinyl monomer added to the polymer backbone.

2. Experimental

2.1. Material and measurements

10-Undecylenoic acid, brilliant yellow, cholesterol and pyridine were purchased from Beijing Chemical Co. Hexachloroplatinic acid hydrate and thionyl chloride were obtained from Shenyang Chemical Co. Poly(methylhydrogeno)siloxane (PMHS) was provided by Merk. Pyridine was purified by distillation over KOH and NaH before using.

Fourier transform infrared spectroscopy (FTIR) of the synthesized polymers and monomers in solid state were obtained by the KBr method performed on a Nicolet 510P FT IR Spectrometer.

Thermal transition properties were characterized by a TA Instruments V2.3C at a heating rate of 10 °C/min under nitrogen atmosphere. Visual observation of LC transitions under cross polarized light was made by a Leitz Laborlux S polarizing optical microscope (POM) equipped with a THMS-600 heating stage.

The photoluminescence (PL) spectra of the monomer and polymers were obtained using a Shanghai Instruments Model-960 Spectrofluorphotometer.

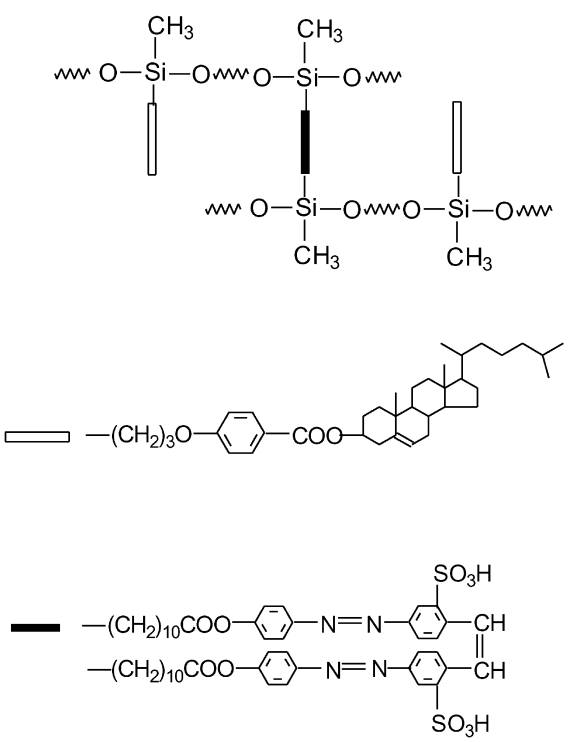

Scheme 1.

Small angle X-ray scattering (SAXS) measurements were performed using Cu Kα ($\lambda = 1.542$ Å) radiation monochromatized with a Ni filter and a totally reflecting glass block (Huber Small-angle Chamber 701). The intensity curves were measured using a linear position sensitive detector (Mbraun OED-50M). The fine focus (0.4×10 mm) X-ray tube is placed in a point-focus position. The beam is reduced in the vertical direction with a 1 mm slit in front of the sample and a triangular slit in front of the detector. The scattering vector lies in the horizontal direction and its length is defined as $q = (4\pi/\lambda) \sin\theta$ (with 2θ being the scattering angle). The background scattering was measured separately and subtracted from the intensity curves.

2.2. Synthesis

2.2.1. Synthesis of 2,2′-(1,2-ethenediyl)-bis[5-[(4-undecenoyloxy)phenyl]-azo]-benzenesulfonic acid

10-Undecylenoic acid (18.4 g, 0.1 mol) and thionyl chloride (25.0 g, 0.21 mol) were added into a round flask equipped with an absorption instrument of hydrogen chloride. The mixture was stirred at room temperature for 2 h, then heated to 60 °C and kept for 3 h in a water bath to ensure that the reaction finished. The mixture was distilled under reduced pressure to obtain 12.4 g 10-undecenoyl chloride at 160–170 °C/20 mm Hg in the yield of 61%.

Brilliant yellow (6.3 g, 0.01 mol) was dissolved in 120 ml pyridine to form a solution. 10-Undecenoyl chloride (4.1 g, 0.02 mol) was added to the solution and reacted at 80 °C for 6 h, cooled, poured in 500 ml of cold water and acidified with 6N H_2SO_4. The precipitated crude product was filtered and recrystallized from ethanol/water (1/1) and dried overnight at 85 °C under vacuum to obtain a brown powder of product in the yield of 70%. Mp: 132 °C.

IR (KBr, cm^{-1}): 3420 (–OH); 3080 (=C–H); 2928, 2856 (CH_3– and $-CH_2$–); 1201 (C–O–C); 1121, 1050 (S=O in $-SO_3H$).

2.2.2. Synthesis of cholest-5-en-3-ol(3β)-4-(2-propenyloxy)benzoate

It was prepared according to previously reported synthetic method [12]. The yield was 60%.

IR (KBr, cm^{-1}): 3050 (=C–H); 2965–2854 (CH_3– and $-CH_2$–); 1735 (C=O); 1606, 1508 (phenyl); 1192 (C–O–C).

2.3. Synthesis of the elastomers

For synthesis of polymers P_0–P_7, the same method was adopted. The polymerization experiments were summarized in Table 1. The synthesis of polymer P_4 was given as an example. 2,2′-(1,2-Ethenediyl)-bis[5-[(4-undecenoyloxy)-phenyl]-azo]-benzenesulfonic acid (0.205 g, 0.220 mmol, monomer A) was dissolved in 150 ml of dry, fresh distilled toluene. To the stirred solution, cholest-5-en-3-ol(3β)-4-(2-propenyloxy)benzoate (4.68 g, 8.56 mmol, monomer B),

Table 1
Polymerization and PL properties

Sample	Feed				Yield (%)	Photolumenscence[a]	
	PMHS (mmol)	*A* (mmol)	*B* (mmol)	*A*/(*A* + *B*) (mol%)		λ_{max} (nm)	Intensity[b] ($\times 10^3$)
P_0	0.3	0	9.00	0	90	–	–
P_1	0.3	0.022	8.96	0.25	90	494	0.10
P_2	0.3	0.045	8.91	0.50	90	494	0.24
P_3	0.3	0.090	8.82	1.00	88	493	0.51
P_4	0.3	0.220	8.56	2.50	87	494	1.03
P_5	0.3	0.429	8.14	5.00	87	493	1.98
P_6	0.3	0.818	7.36	10.0	85	494	4.04
P_7	0.3	4.500	0	100	82	–	–

[a] Obtained from solutions of the samples (0.0050 g) in 50 ml toluene.
[b] Calculated from the peak area by the spectrofluophotometer.

poly(methylhydrogeno)siloxane (0.63 g, 0.30 mmol) and 2 ml of H_2PtCl_6/THF (0.50 g hexachloroplatinic acid hydrate dissolved in 100 ml tetrahydrofuran THF) were added and heated under nitrogen and anhydrous conditions at 65 °C for 72 h. The solvent was removed under reduced pressure, and the crude polymer was purified by precipitation from solution in methanol by the addition of THF. After filtration and evaporation of the solvent, the product was dried at 80 °C for 2 h under vacuum to obtain 5.0 g of polymer in the yield of 90%.

IR (KBr, cm^{-1}): 3440 (–OH); 2960–2850 (CH_3– and –CH_2–); 1738 (C=O); 1603, 1508 (phenyl); 1260 (Si–C); 1190 (C–O–C); 1100–1000 (Si–O–Si).

3. Results and discussion

3.1. FTIR spectra

Polymer P_4 contains the representative features for all of the ionic LC elastomers, their characteristic absorption bands are mentioned above. Fig. 1 shows the FTIR spectrum of ionic LC polymer P_4 recorded at room temperature in KBr pellets. The disappearance of the Si–H stretching at 2160 cm^{-1} indicates successful incorporation of monomers into the polysiloxane chains.

For organic sulfonic acid, the FTIR absorption range of the O=S=O asymmetric and symmetric stretching modes lies in 1120–1230 and 1010–1080 cm^{-1} respectively, and that of the S–O stretching mode lies in 600–700 cm^{-1}. Because of the overlap found for both asymmetric and symmetric stretching bands of SO_2 with C–O and Si–O stretching bands in the polymers under study, the S–>O stretching mode is chosen for identification of sulfur groups in the ionic polymers. Fig. 2 compares the FTIR spectra in the range of 400–900 cm^{-1} for (a) nonionic P_0, (b) 0.5 mol% ionic content P_2, (c) 2.5 mol% ionic content P_4.

While there is no S–O stretching mode found in nonionic content P_0, such a mode is found as a weak band at 636 cm^{-1} for the sample of 0.5 mol% ionic content, and a stronger absorption band is found at 635 cm^{-1} for the sample of 2.5 mol% ionic content P_4. These results clearly indicate successful incorporation of ionic groups, whose concentration increases with an increase in the concentration of ionic monomers containing bright yellow content.

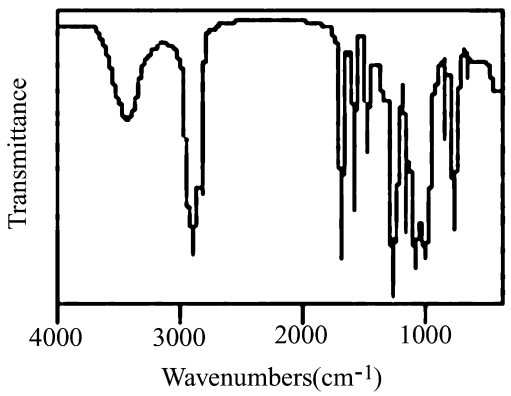

Fig. 1. FTIR spectrum of ionic LC elastomer P_4.

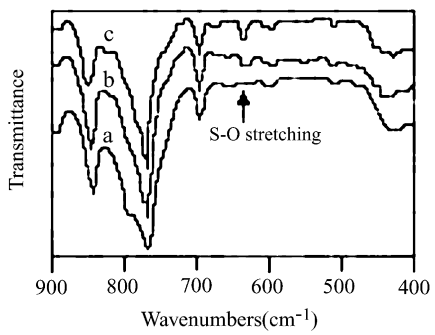

Fig. 2. IR spectra in the range of 400–900 cm^{-1} for (a) nonionic P_0, (b) 0.5 mol% ionic content P_2, (c) 2.5 mol% ionic content P_4.

3.2. PL spectra

Because of the azo groups and the conjugated structure, the ionic crosslinking agent of the elastomers can be analyzed by using PL spectrum. Fig. 3 shows the PL spectra of the elastomers, which were obtained from a solution of the elastomer (0.0500 g) in 50 ml toluene. It is shown that the photoluminescent maxima of the ionic elastomers occur at about 494 nm. The spectra are narrow because of the constant chromophores in the elastomers. The intensities of the peaks increase linearly with increasing ionic monomer concentration in the feed (see Table 1).

3.3. Swelling behavior

The degree of swelling of a polymer network or the volume fraction of polymer in the swollen network is mainly determined by the effective crosslink density (or the molecular weight between the crosslink points (M_c)) and the interaction parameter between the solvent and the network.

Amphiphilic networks exhibit both hydrophilic and hydrophobic properties, so organic/water mixtures were chosen as swelling solvent. The solvents were selected by the percentage swelling of elastomer P_4 in THF/buffer, dimethyl sulfoxide (DMSO)/buffer, acetone/ buffer. The buffer solution of pH 3.1 was made by 0.20 M HAc and 0.004 M NaAc.

Dried networks sample (of approximately 0.2 g each) were placed in the bottom of 20 ml glass bottles. An accurately known large initial volume of a solvent mixture was added. After the bottles were sealed, they were left in a constant temperature insulated box for 2 days. The fully swollen networks were then blotted with filter paper to remove the surface solvent before weighing. The percentage swelling of these samples was defined as (swollen weight/dried weight) × 100%. To determine preferential absorption in solvent mixtures, it was necessary to use smaller volume of solvent in the swelling tests. Fig. 4 shows the swelling behavior for elastomer P_4 in three mixture solvents. It was shown that the swelling ratio of elastomer P_4

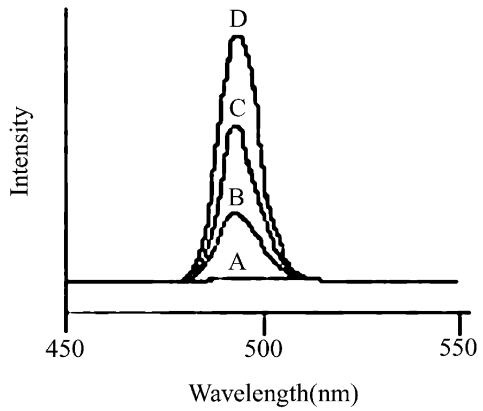

Fig. 3. PL spectra for (A) P_0, (B) P_2, (C) P_4 and (D) P_6 in toluene at the same concentration.

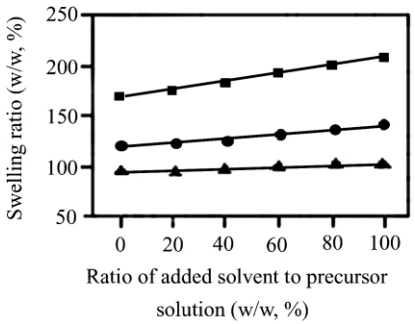

Fig. 4. Swelling ratio (swollen weight/dry weight) of P_4 in different solvents (■) in DMSO/buffer; (●) in THF/buffer; (▲) in acetone/buffer.

is largest for DMSO/buffer, followed by THF/buffer and then acetone/buffer. So the swelling measurements were made in DMSO/buffer solvent.

Swelling measurements were made in 10 ml of DMSO/-buffer mixtures (volume ratio 1/1) with samples of about 0.2 g in initial weight. A buffer solution of desired pH and ionic strength I (0.1 M) was used as a function of solvent composition. The buffer solutions of different pH values were made by Britton–Pobinson method. Swelling was accomplished in several days at room temperature. Swollen elastomers removed from solvents at regular intervals were dried superficially with filter paper, weighed and placed in the same condition. The measurements were continued until a constant weight was reached for each sample.

The equilibrium/swelling ratio of networks was determined gravimetrically through the following equation:

$$Q = 1 + (W_2/W_1 - 1)\rho_p/\rho_s \quad (1)$$

Where Q is the swelling ratio of networks by volume; W_1 is weight of the network before swelling; W_2 is the weight of the network at equilibrium swelling; ρ_p and ρ_s are densities of polymer and solvent, respectively. The volume fraction of polymer network V_{2S} was calculated as

$$V_{2S} = 1/Q \quad (2)$$

The density of the polymer networks was determined in absolute ethyl alcohol by measuring the exact volume of the sample (~1 g). The values of the density of ethyl alcohol and their dependence on temperature were taken from literature [13].

Ionic polymer networks in aqueous solutions yield a more complicated situation than that of neutral polymers. When the networks contain ionizable groups, the forces that influence swelling may be greatly increased. The Flory–Rehner models that describe the molecular weight between crosslinks can only be applied to homogeneous networks [14]. The ionic elastomers do not fall in this category. Brannon–Peppas derived an equation to describe this ionic contribution

Table 2
Some swelling properties of polymers

Sample	Density (g/cm^3)	V (cm^3/g)	V_{2r}	V_{2S}				χ	M_c (g/mol)
				pH 1.9	pH 2.4	pH 3.5	pH 4.5		
P_0	1.063	0.94	–	–	–	–	–	–	–
P_1	1.069	0.94	0.99	0.30	0.30	0.29	0.20	0.614	4800
P_2	1.078	0.93	0.99	0.33	0.33	0.32	0.22	0.624	4000
P_3	1.083	0.92	0.98	0.33	0.33	0.32	0.23	0.630	3500
P_4	1.101	0.91	0.97	0.34	0.34	0.33	0.24	0.636	3000
P_5	1.117	0.90	0.95	0.40	0.40	0.39	0.30	0.656	2500
P_6	1.129	0.89	0.94	0.50	0.51	0.50	0.40	0.739	1200
P_7	1.150	0.87	0.92	–	–	–	–	–	–

term for both anionic and cationic systems [15]:

$$(V_1/4I)[K_a/(10^{-pH}+K_a)]^2(V_{2S}/V)^2 = \ln(1-V_{2S})+V_{2S}+\chi V_{2S}^2+V_{2r}(V_1/VM_c)(1-2M_c/M_n)[(V_{2S}/V_{2r})^{1/3}-(V_{2S}/V_{2r})/2] \quad (3)$$

where M_c is the number average molecular weight between crosslinks; χ is Flory polymer-swelling agent interaction parameter; V_1 is the molar volume of the swelling agent; I is the ionic strength of the swelling medium; K_a is the dissociation constant of ionizable groups on polymer; V is the specific volume of dry polymer; M_n is the number-average molecular weight of the linear macromolecules before crosslinking; and V_{2r} is the polymer volume fraction after crosslinking but before swelling.

Using Eq. (3), we can obtain a linear relation with χ and M_c values as the intercept and inverse slope, respectively, as expressed by Eq. (4)

$$A = \chi + B/M_c \quad (4)$$

The relevant experimental parameters to be used are as follows: $I = 0.1$ M; $V_1 = 28.7$ cm^3/mol; $M_n = 19,000$; p$K_a = 6.0$. The parameter V is calculated by using density values of the polymers. Some of the information about the structural properties of the elastomers was collected in Table 2. By using both the experimentally measured polymer volume fractions V_{2S} of the elastomers in their equilibrium-swollen state and the above-mentioned data, it is possible to establish the corresponding linear relationships as show in Fig. 5. The respective χ and M_c values were determined via linear regression analysis of the lines given in Fig. 5, which are listed in Table 2.

From the results listed in Table 2 one can see that for the ionic network with the lowest amount of crosslinking agents relatively high values for the degree of swelling are found. The value V_{2S} becomes higher for an increasing functionality of the crosslinking agents, corresponding to a higher crosslink density and a lower degree of swelling. It is shown that an increase in the molecular weight between crosslinks increases the swelling of the polymer.

3.4. Liquid-crystalline behavior

All the polymers were studied by DSC and observed by polarizing microscopy, which were summarized in Table 3.

Fig. 6 shows the DSC thermograms of all the polymers synthesized. In the DSC curves, the siloxane soft segment glass transition (T_g) is easily discernible at about 63 °C in the series of polymers. Two kinds of melting temperature (T_m) of the ionic crystalline polymers are clearly detected in P_1, P_2, P_3, P_4 and P_5. The first melting temperature (T_{ms}) corresponds to crystallization of siloxane matrix induced by ionic aggregates. From P_1 to P_5, the values of T_{ms} decrease with increasing crosslinking content, whereas the enthalpy of melting increases. The second melting peak (T_{ml}) corresponds to crystallization of LC segments. The values of T_{ml} are almost constant at 125 °C, and the enthalpy of melting increases from P_0 to P_5. Because endothermic peaks of P_6 and P_7 were very broad, transition temperatures were determined by optical polarizing microscope observations. The anisotropic-to-isotropic transition temperature (T_i) of the polymers is found in P_0–P_5, suggesting that these materials were thermotropic LC polymers. The mesogenic segments were crystalline domains below T_{ml} and were LC domains between T_{ml} and T_i in the siloxane matrix. For P_6

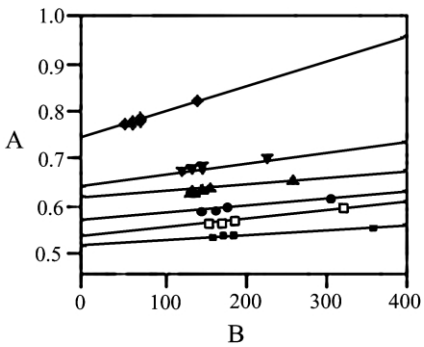

Fig. 5. Determination of χ and M_c values of polymers from swelling data. (■) for P_1; (□) for P_2; (●) for P_3; (▲) for P_4; (▼) for P_5; (◆) for P_6.

Table 3
Characterization of series polymers

Sample	DSC				Optical microscope			Long spacing[a] (Å)
	T_g (°C)	T_{ms}[b] (°C)	T_{ml}[c] (°C)	T_i[d] (°C)	T_{ms}[b] (°C)	T_{ml}[c] (°C)	T_i[d] (°C)	
P_0	63	–	125	235	–	125	236	252
P_1	63	108	126	235	109	125	235	260
P_2	64	108	125	236	108	125	236	245
P_3	62	106	124	228	107	124	230	285
P_4	62	103	125	226	104	125	225	254
P_5	63	101	125	226	101	125	226	232
P_6	64	95	–	–	98	–	–	400
P_7	64	91	–	–	93	–	–	–

[a] Determined for the solid sample prepared by cooling the preceding phase.
[b] Melting temperature of siloxane matrix induced by ionic aggregates.
[c] Melting temperature of crystallization of LC segments.
[d] Meso-to-isotropic phase transition temperature of mosogenic segments.

and P_7, the anisotropic-to-isotropic phase transition could not be detected in the DSC curves, and it was not seen by optical polarizing microscope observations. The liquid-crystal mesophase region decreases slightly with increasing crosslinking content from P_0 to P_5. For polymer P_6 which contain more ionic crosslinking content, the liquid-crystal mesophase disappears.

The optical polarizing microscope observations revealed that the polymers P_0, P_1 and P_2 exhibited smectic mesophase textures. P_3, P_4 and P_5 showed cholesteric mesophase textures. Fig. 7 shows mesophase textures of the representative polymer P_2 and P_3 on first heating. For P_2, when it was heated on the hot stage of the polarizing microscope, a broken focal-conic fan-shaped texture of the smectic phase appeared. When heating to 236 °C, eyeshot become dark demonstrating the anisotropic-to-isotropic phase transition. For P_3, when it was heated, an oily streak texture of the cholesteric mesophase appeared. When heating to 230 °C, the texture disappeared.

Both ionic groups and chemical crosslinking may influence the LC behavior of the elastomers.

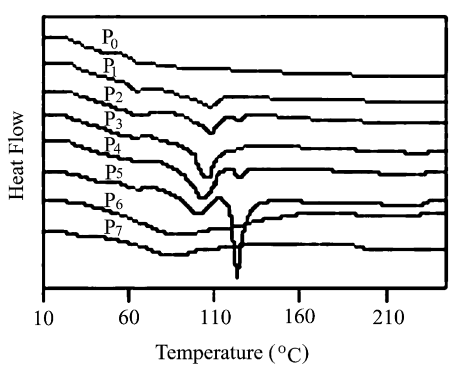

Fig. 6. DSC thermograms of series polymers (on the first heating (10 °C)/min).

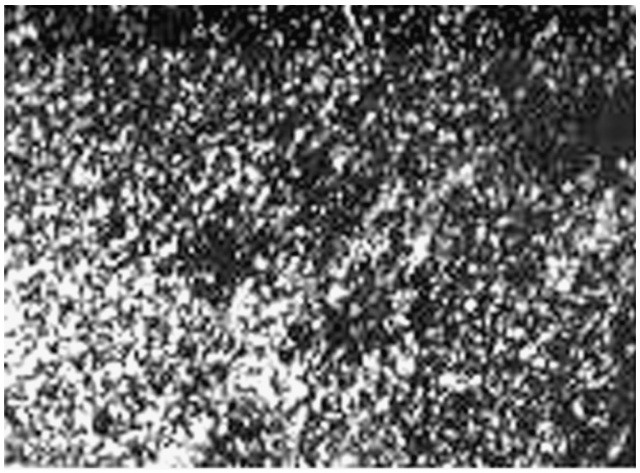

Fig. 7. Optical polarizing micrographs of polymers for (A) P_2 at 165 °C and (B) P_3 at 182 °C on first heating (200 ×).

LC polymers are most commonly composed of flexible and rigid moieties, self-assembly and nanophase separation into specific micro-sructures (often lamellar for side-chain architecture) frequently occur due to geometric and chemical dissimilarity of the two moieties. The majority of side-chain LC polymers such as siloxane polymers are atactic, for such disordered systems low temperatures induce vitrification rather than crystallination. For polymer of this tape, the glass-transition temperature may be considered as a measure of the backbone flexibility. In addition, the nature of the side-group also influences the glass-transition temperature.

Chemical crosslinking imposes additional constrains on the segmental motion of polymer chains, and might be expected to raise the glass-transition temperatures. However, it illustrates a general principle that low level of crosslinking do not markedly effect the phase behavior of

the materials [16]. Crosslinking units may act as a non-mesogenic diluent and destabilize the phase in a manner analogous to the freezing-point depression in liquids. Furthermore, chemical crosslinks in polymers could introduce inhomogeneity in the networks in the form of clustered hard segments.

It is well-known that the incorporation of ionic groups leads to an elevated glass transition temperature for ionomers based on amorphous, flexible polymers [17]. On the other hand, ionic side-chain polymers lead to nano-phase-separated morphologies [18]. For ionomers with a relatively low proportion of ionic units, two-phase behavior is frequently observed due to ionic aggregation in a relatively nonpolar matrix, with consequent reduction in mobility of neighboring nonpolar regions.

In this scheme, at lower ionic contents, ion pairs exist as small ionic aggregates, called multiplets, as well as isolated ion pairs. As the ionic content increases, an ion rich phase, called a cluster phase, begins to form and increases its volume. The cluster phase is considered to be a separate phase [19]. Cluster aggregation in which the ion clusters are completely surrounded with the organic material and actual microseparation of the ionic phase from the siloxane matrix takes place. On the other hand, polymethylsiloxane has low glass transition temperature; the phase separation process should thus be fast because the siloxane matrix has high mobility [20]. Obviously the organization of the longer hard segments is easer, resulting in a higher degree of crystallinity of the hard phase. These results demonstrate the behavior of the siloxane soft segment glass transition (T_g) and the melting temperature (T_{ms}) corresponds to crystallization of siloxane matrix.

In the ionomer literature, the soft and hard phases are also frequently referred to the matrix phase and the cluster phase, respectively. Ionic aggregates or multiplets may be dispersed in the soft or matrix phase. The hard or clusterphase is essentially composed of complex aggregates of multiplets along with a considerable proportion of nonionic material. The ion aggregate in domains due to their electrostatic interactions, thus forcing the siloxane chains to fold and form an irregular lamellar structure. These lamellae are similar to some crystalline–amorphous block copolymers. For LC ionomers, it has shown that ionic clusters are compatible with LC phase. The competition between the formation of ionic clusterphases and LC phases depends on the chemical structure [21]. As shown in Fig. 6, the entropy change at the melting temperature (T_{ml}) increased with increasing ionic crosslinking content for P_0–P_5. This can be explained by the increasing perfection of crystals in the polymers due to the interaction between ionic clusters and LC segments. For P_6, an increased broadening of melting peaks with an increase in the ionic content is seen from DSC thermograms. These results should reflect increased diversity in size and in the arrangement of crystallites, possibly due to increased structural heterogeneity. The ionic cluster lamellae and the LC segments

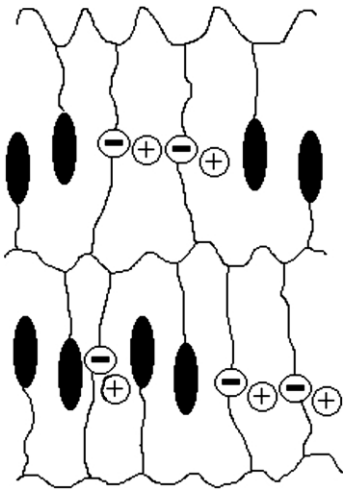

Fig. 8. Schematic representation of lamellar structure containing LC mesogenic units and ionic clusters.

may be dispersed each other to form multiple blocks, leading to the disappearance of liquid-crystal mesophases. These results also demonstrate it is difficulty to observe T_i. A model containing LC segment structure and ionic crosslinking lamellar structure separated by siloxane chains is shown schematically in Fig. 8.

These results are confirmed by SAXS. The scattering peaks were detected in the SAXS profiles of as-cast films of P_0, P_2, P_5 and P_6 as shown in Fig. 9.

The SAXS pattern of all the specimens include clear reflection maxima with a spacing (L) within a range of 200–400 Å, showing that a long period exists in the crystalline polymers. The corresponding data are listed in Table 3. The lamellar spacings are attributed to the stacked lamellar structure with chain foldings [22].

For the polymer P_0, besides intense peak corresponding to a characteristic size of lamellar spacing, a shoulder peak at $q = 1.39\ \mathrm{nm}^{-1}$ is observed, and the derived Bragg

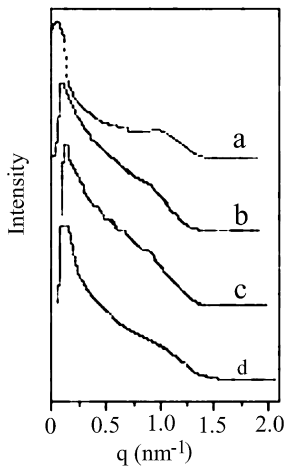

Fig. 9. SAXS patterns collected from the series of polymers for (a) P_0; (b) P_2; (c) P_5; (d) P_6.

spacing (d) is 45 Å. The presence of the shoulder peak at small scattering angles suggests the layered packing of the mesogenic groups. The microstructure of the polymer P_0 is most likely lamellar in nature. In consideration of the thickness of the soft main-chain matrix, the lamellae thickness ($d = 45$ Å) is nearly equal to the fully extended side-chain LC unit (35 Å). The smectic A phase has long range orientational order due to the extended configuration of polymer molecules. Further, it has a one-dimensional positional order with the layer spacing nearly equal to the repeat length of a fully extended polymer. We thus suggest that the polymer P_0 falls in this category. Because chain folding takes place on the crystallization of the polymer, a stacked lamellar structure is formed, leading to an intense peak in the SAXS profile.

For the polymer P_2 which contains a small amount of ionic crosslinking content, the X-ray scattering pattern shows a intense scattering peak at $q = 0.26\ \mathrm{nm}^{-1}$ and a shoulder peak at $q = 0.86\ \mathrm{nm}^{-1}$, which suggests a lamellar structure. The intensity of the principal scattering peak of P_2 is weaker than that of P_0, but the lamellar spacing is similar to that of P_0. This can be explained by the fact that ionic clusters are compatible with LC phase, as shown in Fig. 8.

As shown in Fig. 9, the X-ray scattering pattern of P_5 shows an intense scattering peak at $q = 0.27\ \mathrm{nm}^{-1}$ corresponding to the lamellar spacing. Particularly, there are some shoulder peaks between $q = 0.47\ \mathrm{nm}^{-1}$ and $q = 0.99\ \mathrm{nm}^{-1}$. This result is due to the competition between the formation of ionic cluster phases and LC phases. With the increase of ionic crosslinking content, the formation of ionic clusters is easier in some nanophase, whereas the LC mesogens act as governing factors in other nanophase, leading to a nanophase separation during multiplayer formation.

For P_6, the profile shows an intense peak at $q = 0.16 \times \mathrm{nm}^{-1}$ (corresponding to a lamellar spacing of 400 Å), but the shoulder peak is rather weak. It indicates increased diversity in size and in the arrangement of crystallites, possibly due to increased structural heterogeneity. It suggests that chain foldings is formed easily with increasing ionic crosslinking content, thereby crystallization of the polymer increases.

4. Conclusions

We have synthesized a series of LC elastomers using chemical crosslinking agents containing sulfonic acid groups, which were siloxane-based materials. An ionic divinyl monomer 2,2′-(1,2-ethenediyl)-bis[5-[(4-undecenoyloxy)phenyl]-azo]-benzenesulfonic acid was used as chemical crosslinking agent. Cholest-5-en-3-ol(3β)-4-(2-propenyloxy)benzoate was synthesized as LC monomer. The polymers were prepared in a one-step reaction with ionic crosslinking contents ranging between 0 and 100 mol%. Their chemical structures were determined by various experimental techniques including FTIR and PL spectroscopies. Their LC properties were characterized by DSC, POM and SAXS.

The crosslink densities of the elastomers were determined by swelling experiments. The variety of network structures obtained by varying the ionic crosslinking contents leads to different swelling properties in mixed buffer/organic solvent mixtures. We show that for the ionic network with the lowest amount of crosslinking agents relatively high values for the degree of swelling are found. It is shown that an increase in the molecular weight between crosslinks increase the swelling of the polymer.

Two kinds of melting temperature corresponding to crystallization of siloxane matrix and crystallization of LC segments are clearly detected in some of the ionic crystalline polymers. The optical polarizing microscope observations revealed that the polymers exhibited smectic mesophase textures or cholesteric mesophase textures. Liquid-crystal mesophase region of the polymers become narrow with increasing ionic crosslinking content. A proposed model containing LC segment structure and ionic crosslinking lamellar structure separated by siloxane chains was given. The ion aggregated in domains forces the siloxane chains to fold and form an irregular lamellar structure. The ionic aggregates and LC segments may be dispersed each other to form multiple blocks with increasing ionic crosslinking content, leading to the disappearance of liquid-crystal mesophase.

Acknowledgements

The authors are grateful to the National Natural Scientific Fundamental Committee of China and the prior research program (973) of the Minister of Science and Technology of China for financial support of this work.

References

[1] Kishi R, Sisido M, Tazuke S. Macromolecules 1990;23:3779–84.
[2] Zentel R. Angew Chem Adv Mater 1989;101(10):1437–45.
[3] Loffler R, Finkelmann H. Macromol Chem, Rapid Commun 1990;11:321–8.
[4] Yuan G, Zhao Y. Polymer 1995;36(14):2725–32.
[5] Wiesemann A, Zentel R. Polymer 1992;33(24):5315–20.
[6] Zhao Y, Lei H. Macromolecules 1994;27:4525–9.
[7] Kim JY, Cohen C. Macromolecules 1998;31:3542–50.
[8] Cochin D, Passmann M. Macromolecules 1997;30:4775–9.
[9] Wiesemann A, Zentel R, Lieser G. Acta Polym 1995;46:25–33.
[10] Wilbert G, Zentel R. Macromol Chem Phys 1996;197:3259–70.
[11] Wilbert G, Traud S, Zentel R. Macromol Chem Phys 1997;198:3769–80.
[12] Adms NW, Bradshaw JS, Bayona JM, Markides KE, Lee ME. Mol Cryst Liq Cryst 1987;147:43–60.

[13] Robert CW. CRC handbook of chemistry and physics. 66th ed. Boca Raton, Florida: CRC Press, 1986. pp 267–8.
[14] Flory PJ, Rehner JJ. J Chem Phys 1943;11:521–30.
[15] Brannon-Peppas L, Peppas NA. Chem Engng Sci 1991;46(3): 715–22.
[16] Frederick JD. J Mater Chem 1993;3(6):551–62.
[17] Kukrihara S, Ishii M, Nonaka T. Macromolecules 1997;30:313–5.
[18] Plate NA, Shibaev VP. J Polym Sci, Macromol Rev 1974;8:117–24.
[19] Eisenberg A, Hird B, Moore RB. Macromolecules 1990;23: 4098–103.
[20] Graiver D, Litt M, Baer E. J Polym Sci, Polym Chem Ed 1979;17: 3573–87.
[21] Pabmann M, Zentel R. Macromol Chem Phys 2002;203:363–74.
[22] Tokita M, Osada K, Watanabe J. Liq Cryst 1997;23:453–6.